Preprint *Free Radical Biology and Medicine 2018* https://doi.org/10.1016/j.freeradbiomed.2018.05.006

Kinetic and stoichiometric constraints determine the pathway of H_2O_2 consumption by red blood cells

Florencia Orrico[a,b], Matías N. Möller[b,c*], Adriana Cassina[c,d], Ana Denicola[b,c] and Leonor Thomson[a,c*]

[a]Laboratorio de Enzimología, Instituto de Química Biológica, Facultad de Ciencias, Universidad de la República, 11400 Montevideo, Uruguay. [b]Laboratorio de Fisicoquímica Biológica, Instituto de Química Biológica, Facultad de Ciencias, Universidad de la República, 11400 Montevideo, Uruguay. [c]Center for Free Radical and Biomedical Research, Facultad de Medicina, Universidad de la República, 11100 Montevideo, Uruguay. [d]Departamento de Bioquímica, Facultad de Medicina, Universidad de la República, 11100 Montevideo, Uruguay.

*Corresponding authors: L.T., Laboratorio de Enzimología, Facultad de Ciencias, Universidad de la República, Iguá 4225, 11400, Montevideo, Uruguay. Phone: 598-25258618 ext. 7214. E-mail: lthomson@fcien.edu.uy and M.M., Laboratorio de Fisicoquímica Biológica, Facultad de Ciencias, Universidad de la República, Iguá 4225, 11400, Montevideo, Uruguay. Phone: 598-25258618 ext. 7214. E-mail: mmoller@fcien.edu.uy

Abstract

Red blood cells (RBC) are considered as a circulating sink of H_2O_2, but a significant debate remains over the role of the different intraerythocyte peroxidases. Herein we examined the kinetic of decomposition of exogenous H_2O_2 by human RBC at different cell densities, using fluorescent and oxymetric methods, contrasting the results against a mathematical model. Fluorescent measurements as well as oxygen production experiments showed that catalase was responsible for most of the decomposition of H_2O_2 at cell densities suitable for both experimental settings (0.1-10 x 10^{10} cell L^{-1}), since sodium azide but not N-ethylmaleimide (NEM) inhibited H_2O_2 consumption. Oxygen production decreased at high cell densities until none was detected above 1.1 x 10^{12} cell L^{-1}, being recovered after inhibition of the thiol dependent systems by NEM. This result underlined that the consumption of H_2O_2 by catalase prevail at RBC densities regularly used for research, while the thiol dependent systems predominate when the cell density increases, approaching the normal number in blood (5 x 10^{12} cell L^{-1}). The mathematical model successfully reproduced experimental results and at low cell number it showed a time sequence involving Prx as the first line of defense, followed by catalase, with a minor role by Gpx. The turning points were given by the total consumption of reduced Prx in first place and reduced GSH after that. However, Prx alone was able to account for the added H_2O_2 (50 µM) at physiological RBC density, calling attention to the importance of cell density in defining the pathway of H_2O_2 consumption and offering an explanation to current apparently conflicting results in the literature.

Keywords: Red blood cells, hydrogen peroxide, catalase, peroxiredoxin, glutathione peroxidase, reaction rate, reaction kinetic

Abbreviations: ADP, adenosine diphosphate; ATP, adenosine triphosphate; Cat, catalase; CI, catalase compound I; G6P, glucose 6-phosphate; G6PDH, glucose 6-phosphate dehydrogenase; Gluc, glucose; GPx, glutathione peroxidase; GR, glutathione reductase; GSH, glutathione; GSSG, glutathione disulfide; H_2O_{2Ext}, hydrogen peroxide in the extracellular compartment; H_2O_{2Int}, hydrogen peroxide in the intracellular compartment; Hb Fe^{2+} O_2, oxyhemoglobin; Hb Fe^{3+}, methemoglobin; HK, hexokinase; NADP+, nicotinamide adenine dinucleotide phosphate; NADPH, reduced nicotinamide adenine dinucleotide phosphate; 6PG, 6-phosphogluconate; 6PGDH, 6-phosphogluconate dehydrogenase; 6PGLase, 6-phosphoglucono-lactonase; PGL, phosphogluconolactone; Prx, peroxi-redoxin; $Prx(SH)_2$, reduced peroxiredoxin, Prx-SOH, peroxiredoxin sulfenic acid; Prx(SS), disulfide oxidized peroxiredoxin; Prx-SO_2H, overoxidized peroxiredoxin; R5P, ribulose 5-phosphate; RBC, red blood cells; SOD, superoxide dismutase; TR, thioredoxin reductase; Trx,thioredoxin; TrxSS, oxidized thioredoxin.

Introduction

In circulation, red blood cells (RBC) are exposed to a variable range of H_2O_2 concentrations, that may be high in sites of inflammation [1]. Although the concentration of H_2O_2 in blood is still controversial with currently accepted values in the micromolar range [1], most agree that the main sink of H_2O_2 in the vascular system are the RBC. This is because of various factors, including a high membrane permeability to H_2O_2 and the presence of very efficient H_2O_2-detoxification systems [2]. Red blood cells have several systems that can remove H_2O_2, including peroxiredoxin 2 (Prx), glutathione peroxidase (Gpx) and catalase (Cat) (Figure 1). However, the relative importance of each of these systems is still under debate. On one hand, Low et al. found that Prx in RBC was rapidly oxidized to the disulfide dimeric form in the presence of H_2O_2 that would then slowly reduce back via thioredoxin/thioredoxin reductase/NADPH system , proposing that Prx2 does not behave as a classical enzyme in H_2O_2 trapping [3] . The nearly diffusion-controlled rates for the reaction with H_2O_2 ($k = 1 \times 10^8$ M^{-1} s^{-1}, [4]) and its high abundancy in RBC (240-520 μM) [5–7] suggest that it should be the main protein metabolizing H_2O_2.

On the other hand, Johnson et al. found that deleting the gene for Prx2 in mice did not make the RBC more sensitive to oxyhemoglobin oxidation. Catalase deficient cells were more sensitive to H_2O_2, and the simultaneous deletion of both Cat and Gpx lead to an even

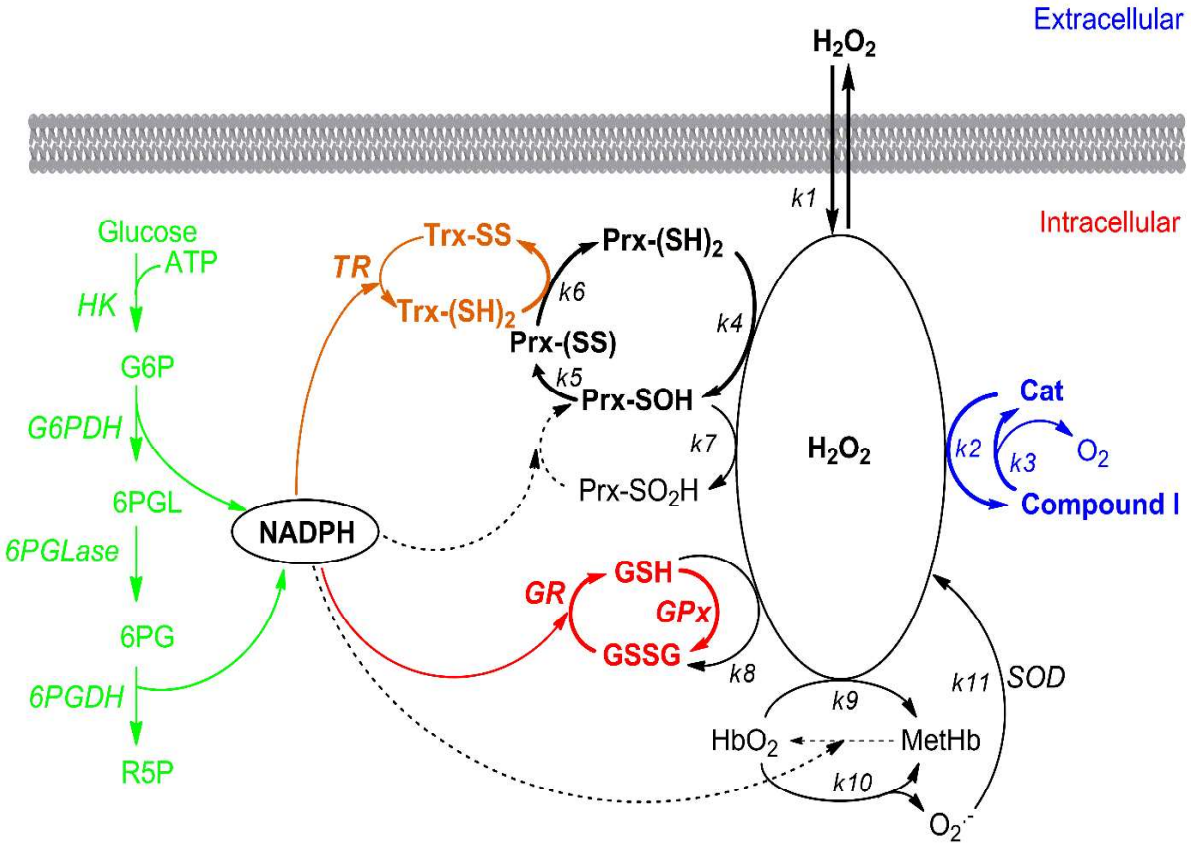

Figure 1. Metabolism of H_2O_2 by RBC. The different processes involved in H_2O_2 metabolism in RBC are depicted, including direct reactions indicated by k# (rate constants in Table 1), and enzyme-catalyzed reactions indicated by the corresponding enzyme (i.e. TR, Dalziel's parameters in Table 2). All these reactions were included in the mathematical model, except for the reactions depicted by dashed arrows which are of scarce relevance in the final model. The most important processes are shown in bold, such as the permeation of extracellular H_2O_2 across the plasma membrane. Catalase is shown in blue (Cat), the peroxiredoxin cycle in black ($Prx-(SH)_2$), the glutathione peroxidase system in red (Gpx), the thioredoxin system in orange ($Trx-(SH)_2$) and the pentose phosphate contributing to NADPH in green. The full name of each component is given in the list of abbreviations.

higher sensitivity [8]. They did notice an increase in intracellular H_2O_2 in Prx2 deficient RBC by measuring the inactivation of Cat with aminotriazole, proposing that Prx2 participated in endogenous H_2O_2 consumption but not in exogenous H_2O_2 removal, and suggesting that the role of this enzyme in erythrocytes might be more important as chaperone during hematopoiesis than as antioxidant in mature cells [8]. Furthermore, Benfeitas et al. built a mathematical model considering all the reactions involved in H_2O_2 metabolism in RBC validated using previously published experimental results. To reconcile the model with experimental results, they proposed the formation of an inactive Prx complex, resulting in an enzyme with an activity comparable to Cat [9].

Herein, with the aim of clarifying the relative importance of the different antioxidant systems in H_2O_2 metabolism, experiments were performed using human RBC exposed to bolus addition of H_2O_2 and the evolution of oxygen derived from catalase activity and the rate of disappearance of H_2O_2 by a fluorimetric method were followed at different cell densities. A mathematical model was built to represent all the possible reactions related to H_2O_2 metabolism in RBC using known rate constants from the literature and adjusting some parameters according to the experimental conditions. The model successfully represented the experimental results and provided further details that showed that the relative importance of each enzymatic system depends on several factors, including the timescale of the experiment, the cell density and the relative concentration of H_2O_2. This complexity may explain the conflicting views in RBC metabolism of H_2O_2 in the literature.

Materials and methods

Chemicals were obtained from Sigma, AppliChem and Acros organics. Spectrophotometric measurements were performed in a Varioskan Flash (Thermo Scientific, Finland) plate reader. High-resolution respirometry studies were done using an OROBOROS Oxygraph-2k (Oroboros Instruments Corp., Innsbruck, Austria).

Cell extraction and preservation. Blood was obtained from volunteer donors after informed consent at the *Cátedra y Departamento de Medicina Transfusional*, Hospital de Clínicas, Facultad de Medicina, Universidad de la República, Uruguay. The research protocol was approved by the Hospital´s Ethics Committee. A total of five blood samples from healthy male volunteers (age 36 ± 11 years) were processed. Packed RBC were obtained by standard techniques without leukoreduction, as described before [10]. Briefly, total blood (450 mL) was collected in primary bags containing 63 mL of anticoagulant solution CPD (129 mM dextrose, 105 mM citrate and 16 mM phosphate, Terumo Corporation, Tokyo, Japan), centrifuged using a Roto Silenta 63RS transfusion bag centrifuge (Hettich, Germany) at 2.200 rpm at 20° C to remove plasma and platelets. Packed RBC were preserved at 4° C in the presence of 100 mL isotonic solution SAGM containing sodium chloride (8.77 g/L), glucose monohydrate (9 g/L), mannitol (5.25 g/L) and adenine (0.3 g/L) (OPTISOL, Terumo Corporation, Tokyo, Japan). The cells were used fresh, immediately after release from the blood bank.

Measurement of H_2O_2 consumption. Intact RBC were incubated in the presence of 50 µM H_2O_2 and the remaining oxidant was measured as previously described [10], with minor modifications. Briefly, the cells (5 x 10^8-1 x 10^{10} cells L^{-1}) were incubated in a 96 well plate (Greiner Bio-One GmbH, Germany) in the presence of 50 µM H_2O_2 in Hank´s balanced salt solution (HBSS), containing 0.137 M NaCl, 5.4 mM KCl, 0.25 mM Na_2HPO_4, 1 g L^{-1} glucose, 0.44 mM KH_2PO_4, 1.3 mM $CaCl_2$, 1.0 mM $MgSO_4$, 4.2 mM $NaHCO_3$, pH 7.4 at 37° C. The consumption of H_2O_2 by RBC was stopped every 2 min by addition to consecutive wells of 100 µL of a mixture containing 10 mM p-hydroxyphenylacetic acid (pHPA) and 0.1 g L^{-1} horseradish peroxidase (HRP) in phosphate buffered saline (PBS) containing 140 mM NaCl, 2.7 mM KCl, 10 mM Na_2HPO_4, 1.8 mM KH_2PO_4, pH 7.4 (stop solution). The fluorescent pHPA dimer formed in the presence of H_2O_2 and HRP was measured (λex = 345 nm, λem = 425 nm) using a plate reader (Varioskan, Thermo, Finland). The concentration of the remaining H_2O_2 was calculated from a standard curve performed under the same conditions using known concentrations of H_2O_2 (2-50 µM). The absorbance at 240 nm (ε = 39.4 $M^{-1}cm^{-1}$) was used to ascertain the concentration of

H_2O_2 [11]. The apparent first-order rate constant for the removal of H_2O_2 (50 µM) by intact RBC (k_{obs}) was determined by nonlinear regression, using equation 1.

$$Y = (Y_0 - Y_{MAX})\, e^{-k_{obs}\, t} + Y_{MAX} \qquad (1)$$

The slope of the secondary plot of k_{obs} against cell number was used to determine k_{cell}.

Evaluation of catalase activity by High-Resolution Respirometry. The oxygen generation from H_2O_2 in the presence of RBC was determined by high-resolution respirometry using an OROBOROS Oxygraph-2k (Oroboros Instruments Corp., Innsbruck, Austria). Basal oxygen was measured for 5 min in the presence of the appropriate number of cells in HBSS under continuous stirring at 37° C. After addition of 50 µM H_2O_2 to the cell suspension the production of oxygen was measured for 20 additional minutes. No significant hemolysis or oxyhemoglobin oxidation was observed under these conditions.

Inhibition of catalase and the thiol-dependent systems. Before the analysis of oxygen production, the cells were incubated for 30 min at 37° C in the presence of sodium azide (2 mM) and NEM (50 mM) to inhibit catalase and the thiol dependent systems, respectively. The effect of sodium azide (2 mM) on the oxygen production by 2 µM of catalase from bovine liver (Sigma-Aldrich Inc., St Louis, MO) and 50 µM H_2O_2 was assayed as positive control.

Computational methods. The model was built in COPASI [12]. It contained two compartments, an extracellular compartment with volume Vol_{ext} where H_2O_2 was added and an intracellular compartment of volume Vol_{int} containing enzymes and metabolites. The volume of the intracellular compartment was calculated using equation 2:

$$\mathrm{Vol_{int}} = \mathrm{Vol_{RBC}} N \qquad (2)$$

where the cell volume (Vol_{RBC}) is 9 x 10^{-14} L $cell^{-1}$ [13,14] , and N the cell number assayed.

The extracellular volume was calculated as depicted in equation 3.

$$\mathrm{Vol_{ext}} = 1 - \mathrm{Vol_{int}} \qquad (3)$$

Table 1. Mass action rate constants used for simulations.

Reaction	Rate constant	References
1	17 s^{-1}	This work
2	6x10^6 M^{-1} s^{-1}	[15]
3	1.6x10^7 M^{-1} s^{-1}	[15]
4	1x10^8 M^{-1} s^{-1}	[4]
5	0.64 s^{-1}	[16]
6	2.1x10^5 M^{-1} s^{-1}	[4]
7	1.2x10^4 M^{-1} s^{-1}	[17]
8	140 M^{-1} s^{-1}	[18]
9	100 M^{-1} s^{-1}	[19]
10	4.5X10^{-7} s^{-1}	[19]
11	6x10^9 M^{-1} s^{-1}	[19]

The reactions are shown in Figure 1.

The rate of the movement of H_2O_2 between both compartments was modeled as indicated by the authors of the software [12] using equation 4.

$$\mathrm{r} = \mathrm{k_{diff}}\, \mathrm{Vol}_{int}\, [\mathrm{H_2O_2}] \qquad (4)$$

where Vol_{int} is the intracellular volume and k_{diff} is a constant representing the rate of H_2O_2 diffusion through the membrane. This constant was determined experimentally (Table 1, Fig. 2).

All the reactions considered for modeling H_2O_2 metabolism in RBC are shown in Figure 1 and further described in Supplementary Material. Individual enzymatic steps for Prx and Cat, as well as uncatalyzed reactions were treated as governed by mass action kinetics (Table 1) [20]. Enzyme catalyzed reactions were modeled using Michaelis–Menten kinetics (Table 2). Time course simulations were performed using COPASI 4.19 [21]. The initial concentrations of all the species involved are shown in Table 3. The parameters for the model were either derived from published work or estimated from our experimental results, as shown in Tables 1-3. Concentration changes over time were expressed as the ratio between the concentration at

Table 2. Dalziel´s parameters used for simulations.

Enzyme	Dalziel's parameters				References
	ϕ_0 (s)	ϕ_1 (Ms)	ϕ_2 (Ms)	$\phi_{1,2}$ (Ms^2)	
TR	NA	$1.35x10^{-6}$	$3.24x10^{-7}$	NA	[22]
Gpx	NA	$2.4x10^{-8}$	$2.5x10^{-5}$	NA	[22–25]
GR	NA	$3x10^{-7}$	$4x10^{-8}$	NA	[26–28]
HK	$4.7x10^{-3}$	$4.7x10^{-6}$	$2.2x10^{-7}$	$1.0x10^{-12}$	[29,30]
G6PDH	$3.6\ 10^{-3}$	$2.6x10^{-8}$	$1.9x10^{-7}$	$5.0x10^{-15}$	[29]
6PGLase	$2x10^{-2}$	$1.8x10^{-6}$	NA	NA	[29]
6GPD	4.6	$1.3x10^{-4}$	$9x10^{-5}$	$1.2x10^{-8}$	[31,32]

NA, not applicable.

each time over the initial concentration of the metabolite (C_t/C_o).

Dummy terms were incorporated into the reactions that reported how much H_2O_2 was consumed by each pathway and were named Q_{Prx}, etc. Therefore, at a given time, total consumed H_2O_2 (Q_T) equals the sum of consumed H_2O_2 by every route:

$$Q_T = Q_{Prx} + Q_{Prx\text{-}SO} + Q_{Cat} + Q_{GPx} + Q_{GSH} + Q_{Hb} \quad (5)$$

And the fraction of H_2O_2 consumed by each system at any time is given by:

$$Fraction(x) = Q_X / Q_T \quad (6)$$

Copasi files are provided as supporting material. All graphics and further analysis of the simulation were performed using GraphPad Prism 6 (GraphPad Software, La Jolla, CA)

Statistical analysis. Data were analyzed using Graphpad Prism 6 (GraphPad Software, La Jolla, CA). Statistical analyses were performed by two-way analysis of variance (ANOVA) and Tukey's post hoc to perform multiple comparison test. Differences with $p<0.05$ were considered statistically significant.

Table 3. Concentrations used in simulations.

Compound	Intracellular concentration (M)	References
ADP	3×10^{-4}	[30]
ATP	2.1×10^{-3}	[30]
Cat	11×10^{-6}	This work
Cl	0	
G6P	3.6×10^{-4}	[45]
G6PDH	9.3×10^{-8}	[33]
Glc	5×10^{-3}	[19]
GPx	1.4×10^{-6}	[34]
GR	1.25×10^{-7}	[33]
GSH	1.5×10^{-3}	[10]
GSSG	2×10^{-8}	[10]
H_2O_{2Ext}	5×10^{-5}	
H_2O_{2Int}	0	
Hb Fe^{2+} O_2	2×10^{-2}	[35]
Hb Fe^{3+}	1×10^{-4}	[35]
HK	1.63×10^{-8}	[33]
$NADP^+$	2×10^{-6}	[36]
NADPH	5×10^{-5}	[36]
6PG	2.7×10^{-5}	[30]
6PGDH	2.1×10^{-6}	[33]
6PGLase	1.4×10^{-7}	[33]
PGL	1×10^{-7}	[33]
$Prx(SH)_2$	4×10^{-4}	[5]
Prx-SOH	0	
Prx-(SS)	0	
$Prx\text{-}SO_2H$	0	
R5P	1×10^{-5}	[33]
SOD	2×10^{-6}	[37]
TR	1.25×10^{-7}	[38]
Trx	9×10^{-6}	[38]
TrxSS	0	

Results

Hydrogen peroxide consumption by red blood cells

To understand the effect of the cell density on H_2O_2 removal by RBC, the rate of H_2O_2 consumption was assayed at different cell densities measuring the fluorescence of pHPA dimer generated in the presence of HRP (Fig. 2). To comply with the requirements of the technique [10,39] the number of cells was relatively low ($0.7\text{-}10 \times 10^9$ cell L^{-1}) as compare with the regular number of RBC inside the circulatory system (5×10^{12} cell L^{-1}) and the concentration of H_2O_2 relatively high

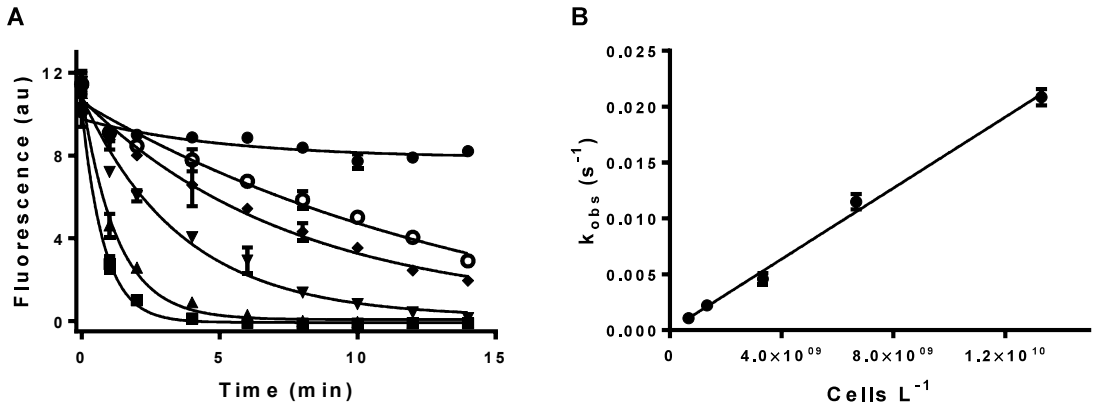

Figure 2. Impact of cell density on H_2O_2 consumption by RBC. A. The rate of H_2O_2 (50 µM) decomposition by RBC at 7 x 10^8 (○), 1 x 10^9 (♦), 3 x 10^9 (▼), 7 x 10^9 (▲) 1 x 10^{10} cells/L (■) was assayed in the presence of pHPA/HRP at 37° C. The same amount of H_2O_2 was analyzed in the absence of cells (●). The results were analyzed by nonlinear regression (Eq. 1) and k_{obs} were obtained. **B.** A k_{cell} of 1.1 ± 0.1 x 10^{-12} $cell^{-1}$ L s^{-1} was determined using the k_{obs} obtained by nonlinear regression from three independent experiments performed as the one shown in figure A with RBC from different donors.

(50 µM). The rate of H_2O_2 consumption was directly proportional to the cell number and a k_{cell} of 1.1 ± 0.1 x 10^{-12} cell L^{-1} s^{-1} was determined, in good agreement with previous reports [10,39]. Under these conditions, sodium azide completely inhibited the consumption of H_2O_2 by RBC (Fig. 3). Conversely, the rate and the total amount of H_2O_2 consumed by the cells remained almost unchanged after pretreatment of the RBC with 50 mM NEM (Fig. 3), indicating a minor role of the thiol dependent systems under these conditions. Although these results may seem surprising when considering that RBC contain 400 µM Prx and GSH in mM concentrations [5,10], these experiments were done at low cellular densities, hence the amount of Prx and GSH in the total volume is actually very low. Because of that both thiol-dependent antioxidants are rapidly oxidized, accounting for a very small fraction of the total H_2O_2 consumed. Since catalase does not need any reducing substrates it can therefore cope with the excess of H_2O_2, becoming the main enzyme responsible for H_2O_2 consumption under these experimental conditions.

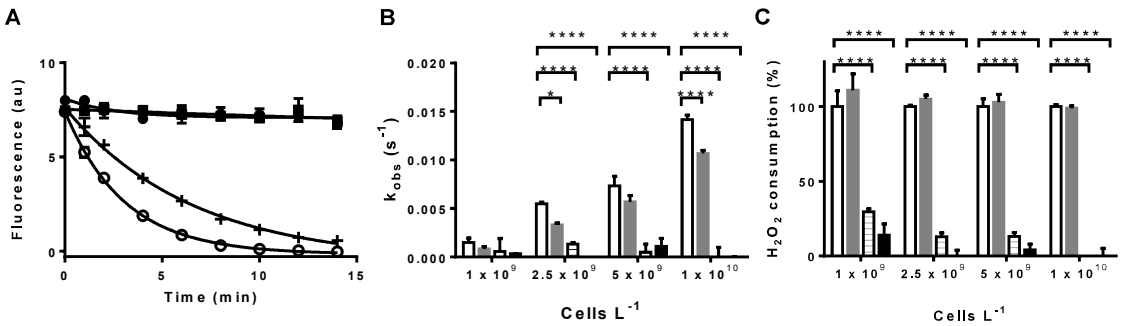

Figure 3. Effect of enzyme inhibitors on the rate of H_2O_2 consumption by RBC. A. Representative time course of H_2O_2 consumption by 3.3 × 10^9 cells L^{-1} incubated for 30 min in the absence (○) and the presence of 2 mM sodium azide (●), 50 mM NEM (+), and sodium azide (2 mM) plus NEM (50 mM) (■). **B.** k_{obs} obtained from non-linear curve fit of the results from experiments performed as in A with 1 x 10^9-1 x 10^{10} cells L^{-1} incubated in the absence (empty bars) and the presence of 50 mM NEM (grey bars), 2 mM sodium azide (dashed bars) and 50 mM NEM plus 2 mM sodium azide (black bars) for 30 min before the addition of 50 µM H_2O_2. **C.** Percentage of H_2O_2 consumed after 15 min by cells treated as in B. Asterisks depict statistically significant differences obtained by 2-way ANOVA followed by Tukey's multiple comparisons test (*p<0.05; **** p<0.0001).

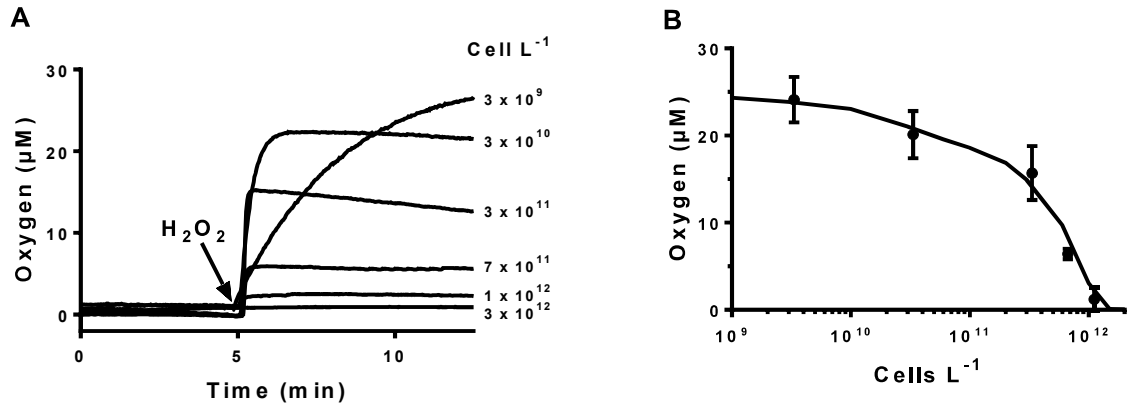

Figure 4. Production of oxygen from H_2O_2 by RBC. A. Oxygen concentration was measured in the presence of 3×10^9, 3×10^{10}, 3×10^{11}, 7×10^{11}, 1×10^{12}, and 3×10^{12} cell L^{-1} before and after the addition of 50 µM H_2O_2 (arrow). **B.** Correlation between oxygen production and cell density. The dots represent maximal oxygen production at each cell density while the line was obtained by simulations performed as described below.

Oxygen production from H_2O_2 and RBC

Another strategy to investigate the participation of the antioxidant systems in RBC was to analyze the release of oxygen from the reaction of intracellular catalase with H_2O_2, using a high-resolution oxygen electrode. Catalase reacts with two molecules of H_2O_2 to produce one molecule of O_2. At low cell densities (≤2 x 10^{10} cel L^{-1}) catalase removed most H_2O_2 added since 22 ± 1 µM O_2 was generated from 50 µM H_2O_2 (Fig. 4A). With increasing cell numbers the rate of oxygen production increased while the total amount of oxygen generated decreased, achieving a minimal value (*x*-intercept) at 1.1 x 10^{12} cells L^{-1} (Fig. 4B), being this cell density the breaking point for catalase mediated H_2O_2 consumption. This result suggest that the consumption of H_2O_2 shifted from catalase to other peroxidase systems as the cell number increased. Supporting this hypothesis, the production of oxygen by 3 x 10^9 cell L^{-1} and 50 µM H_2O_2 was inhibited by sodium azide (2 mM)

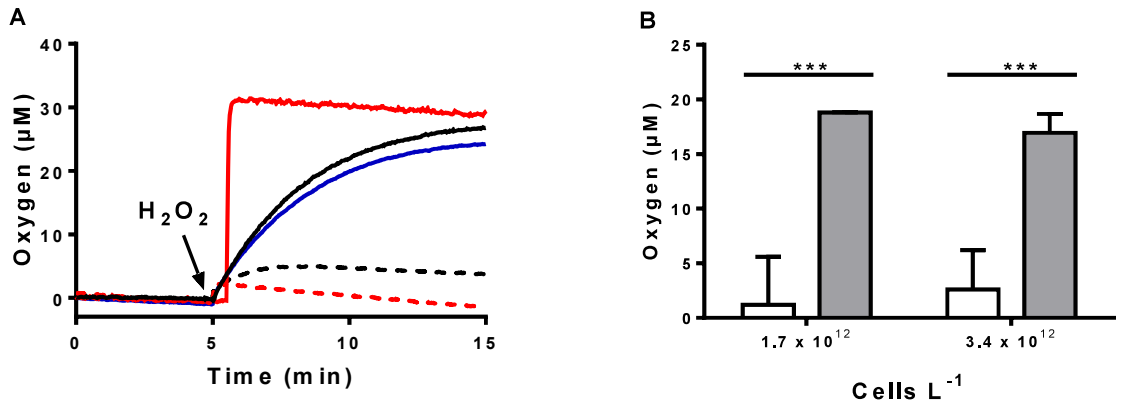

Figure 5. Effect of enzyme inhibitors. A. Representative polarographic oxygen production profile obtained after the addition of 50 µM H_2O_2 (arrow) to 3 x 10^9 cell L^{-1} (black lines) or to an equivalent amount of catalase (2 µM, red lines). Both, cells and catalase were pre-incubated for 30 min at 37° C in the absence (continuous lines) or presence (dashed lines) of 2 mM sodium azide. Oxygen evolution from cells pre-treated in the same condition with 50 mM NEM (continuous blue line) is also shown. **B.** Oxygen production by 1.7 x 10^{12} cells L^{-1} and by 3.4 x 10^{12} cells L^{-1}, pre-incubated in the absence (white bars) and the presence (grey bars) of 50 mM NEM (*** $p<0.001$).

in the same way as it affected the activity of authentic catalase (2 µM), whereas the production of oxygen remained unaffected in the presence of 50 mM NEM (Fig. 5A). In contrast, when the preparations showing minimal oxygen production due to the presence of cell numbers higher than 1.1 x 10^{12} cell L^{-1} (1.7 and 3.4 x 10^{12} cell L^{-1}) were treated with NEM (50 mM) the oxygen generation increased significantly (Fig. 5B). This result indicates that the thiol-dependent systems are responsible for H_2O_2 consumption as the cell density approaches the normal circulatory hematocrit (5 x 10^{12} cell L^{-1}). Therefore, depending on the cell density, different enzymatic systems are responsible for the removal of H_2O_2 by RBC.

Modeling the metabolism of H_2O_2 in RBC

To better understand this complex enzyme system depicted in Figure 1, the consumption of H_2O_2 (50 µM) was simulated using the rate parameters and concentrations shown in Tables 1-3. Some parameters were determined experimentally. For Cat, an intracellular concentration of 11 µM was obtained from kinetic experiments performed as in Fig. 2. Oxymetry results were then used to adjust the concentration of intracellular Gpx and Prx. The oxygen profile was very sensitive to the amount of the different antioxidant systems, with particular effects. The amount of Prx controlled how steep the O_2 evolution decreased with cell density, whereas the amount of Gpx introduced a dip at 10^{10} cells L^{-1}. The best fit was given by 1.5 µM Gpx and 400 µM Prx (Fig. 4B), matching reported values [5,40]. The diffusion constant across the membrane (k1 in Table I) was obtained by fitting results from experiments at low cell density (Figure 2) with the model. In this case it was found that k_1 = 17 s^{-1} (Table 1). After setting these parameters the model was able to reproduce the results obtained at both low and high cell densities, supporting the validity of the model at all the cell densities of interest.

Using the cell density regularly employed in the pHPA/HRP experimental system, 3 x 10^9 cell L^{-1}, the simulated concentration of H_2O_2 decreased exponentially in the extracellular compartment with a rate constant of 4 x 10^{-3} s^{-1} (Fig. 6A), in concordance with the experimental results shown in Fig. 2. The simulation shows that in the intracellular compartment the concentration of H_2O_2 remained constant at sub-micromolar concentration for the initial 0.4 s. The end of this steady phase coincided with the total consumption of the reduced form of both Prx and Trx, triggering a rapid increase of intracellular H_2O_2 in the next 0.2 s, followed by a steady phase that ended at ~1 s supported in part by the recycling of GSH by NADPH, ending with the total consumption of GSH and NADPH in less than 100 s (Fig. 6B). The maximal concentration of H_2O_2 in the intracellular compartment reached 6.7 x 10^{-6} M at ~2 s, while at the same time point the concentration of extracellular H_2O_2 was at least 7 times higher, in agreement with previous reports about the effective scavenging of H_2O_2 by intracellular antioxidants [41]. Finally, intracellular H_2O_2 decreased exponentially with a rate constant of 4 x 10^{-3} s^{-1} (Fig. 5B). This last part involved most H_2O_2 consumption (>97%) and it was mediated by catalase, while the contribution of Gpx and Prx were minimal (2.3 and 0.4%, respectively) (Fig. 6C).

At cell densities higher than 10^{10} cell L^{-1} the rate of H_2O_2 disappearance was too high to be analyzed by the fluorescent method. However, measurements of the catalase-mediated oxygen production were feasible even at cell densities approaching 10^{12} cell L^{-1} (Fig. 4B). *In silico* analysis of oxygen production using 50 µM H_2O_2 and variable cell densities coincided closely with experimental results as depicted in Figure 4, reinforcing the validity of our mathematical model.

An intermediate cell density (3 x 10^{11} cell L^{-1}) was chosen to illustrate the transition between the different intraerythrocytic H_2O_2-metabolizing systems. In an analogous way as with the lower number of cells, with 3 x 10^{11} cell L^{-1} the initial concentration of intracellular H_2O_2 was kept at a very low level during the initial ~0.5 s (Fig. 6D). This low level of oxidant was due to the consumption by the Prx/Trx system, since after the almost simultaneous oxidation of both components the intracellular concentration of H_2O_2 raised steeply, achieving a maximal value in 0.6 s of 4.9x10^{-6} M (Fig. 6E). This abrupt increase was followed by the exponential decay of H_2O_2 (k = 0.46 s^{-1}) accompanying the partial oxidation of GSH and NADPH. After H_2O_2 disappearance, the reduced form of GSH, Prx and Trx recovered gradually, showing that the

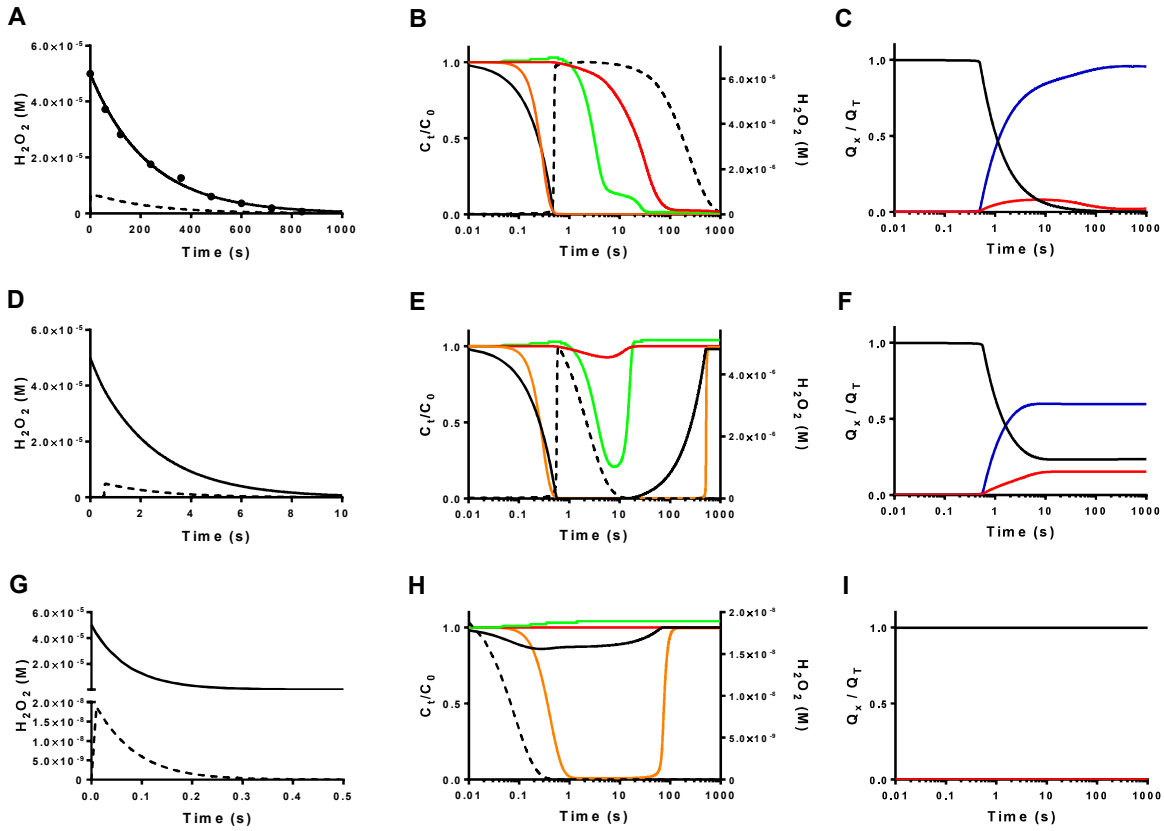

Figure 6. Simulated effect of cell density on H_2O_2 consumption. The consumption of 50 µM of H_2O_2 was simulated in the presence of 3.3 x 10^9 (**A-C**), 3 x 10^{11} (**D-F**) and 5 x 10^{12} cell L^{-1} (**G-I**). **A, D and G**. Consumption of H_2O_2 in the intracellular (dashed line) and extracellular compartment (continuous line). In **A**, symbols represent experimental results from Fig. 1. **B, E and H**. Adjusted concentration (C_t/C_0) of Prx (black line), GSH (red line), NADPH (green line), Trx-SH_2 (orange line), and intracellular concentration of H_2O_2 (black dashed line). **C, F, and I**. Fraction of H_2O_2 (Q_X/Q_T) consumed by Prx2 (black line), Gpx (red line) and catalase (blue line) as a function of time.

prevalence of catalase at low cell number was due to limitations in the recycling rate of the thiol dependent systems (Fig. 6E). In this case Prx and Gpx accounted for 24 and 15% of the total H_2O_2 consumption, respectively; while catalase consumed the remaining 61% (Fig. 6F).

Since the rate of H_2O_2 consumption in the presence of a cell number equivalent to the intravascular density (5 x 10^{12} cell L^{-1}) was too high to be experimentally measured, the results at this cell density are based mainly in the already tested mathematical model. In this case the intracellular concentration of H_2O_2 showed a rapid monophasic increase to 2 x 10^{-8} M in less than 0.001 s, followed by an exponential decrease (k = 13 s^{-1}), accompanying closely its extracellular disappearance (Figure 6G). The consumption of H_2O_2 was concomitant with the fast oxidation of Trx. After that, reduced Trx was reconstituted in less than 2 min, without perturbing the steady state concentration of NADPH (Fig. 6H). This result pointed to the participation of a single antioxidant system, being Prx the exclusive enzyme responsible for H_2O_2 removal (Fig. 6I), coincident with the absence of oxygen production at high cell densities described before.

Hyperoxidation of Prx to sulfinic acid was marginal (≤ 1%) at 50 µM H_2O_2 under the three analyzed cell densities, consistent with experimental results reported previously [3]. The participation of

hemoglobin was minimal, in agreement with its low reaction rate with H_2O_2, accounting for less than 2% of H_2O_2 consumption at <1 x 10^{12} cell L^{-1}, being its role even lower at more physiological cell numbers (not shown).

Considering the fraction of the initial H_2O_2 removed by each system, represented as Q_x/Q_T in Figure 7A, at cell densities below 5 x 10^{11} cell L^{-1} catalase was responsible for most of the H_2O_2 consumption, with a minor contribution from the Gpx/GSH/GR system. The latter contributed up to 15% H_2O_2 consumption at intermediate cell numbers (0.6-3 x 10^{11} cell L^{-1}). Below 1 x 10^{10} cells L^{-1}, catalase consumed more than 95 % of the total H_2O_2. As the cell number increased, catalase was progressively out competed by Prx with a minimal participation at cell densities above 1 x 10^{12} cell L^{-1} (Fig. 7A), in concordance with the absence of oxygen production described above (Fig. 4). At cell densities higher than 1 x 10^{12} cell L^{-1} Prx was practically the exclusive enzyme responsible for H_2O_2 reduction (Fig. 7A). Even though the profiles in Figure 7A correspond to the different antioxidant systems coping with 50 µM, similar profiles are observed at different H_2O_2 concentrations. Figure 7B illustrates the transitions induced by both the cell density as well as the initial concentration of H_2O_2 on the amount of H_2O_2 metabolized by each enzyme system. While catalase-mediated H_2O_2 consumption predominates at low cell densities and high H_2O_2 concentrations, under the inverse condition (i.e. high cell densities and low H_2O_2 concentrations) Prx is the main enzyme responsible for H_2O_2 metabolism. Our experiments and simulations were performed at a concentration of H_2O_2 (50 µM) appropriate to witness the transition between the different antioxidants brought by variations in the number of cells. These transitions can be observed in Figure 7B by following the horizontal dashed line traced at 50 µM H_2O_2. The cell density at the breaking point between catalase and Prx determined at 50 µM H_2O_2 coincided using both simulations (the crossing point between the dashed lines in Fig. 7B) and oxygen consumption experiments (the x axis intercept in Fig. 4B), corresponding to 1.1 x 10^{12} cell L^{-1}.

Discussion

Due to permanent transit across the circulatory system, RBC are continuously exposed to variable conditions, including mechanic as well as chemical stresses. The highly efficient antioxidant machinery of RBC can be taken as a proof of the participation of these cells as real sinks of H_2O_2 in the circulatory system.

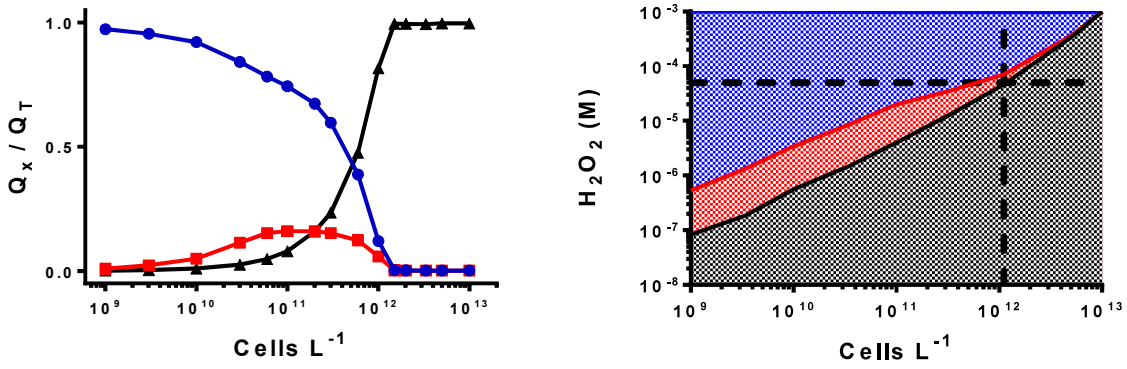

Figure 7. Effect of cell density on H_2O_2 consumption by RBC. A. The fraction of H_2O_2 consumed by every antioxidant system (Q_x/Q_T) (catalase, blue; Prx, black; Gpx, red) were calculated using equations 18-19, from simulations performed for different cell densities (1 x 10^9-1x10^{13} cell L^{-1}) and using dummy values (Q_x and Q_T) obtained after 10 lifetimes of H_2O_2 consumption. **B.** The maximum concentration of H_2O_2 that can be consumed by Prx (black line), Gpx (red line) and catalase (blue line) was simulated at different cell densities. The black dashed area indicates the experimental space where Prx in RBC can be studied; the red dashed area indicates where GPx will be most active and the blue dashed area indicates the conditions under which catalase will be the main enzyme consuming H_2O_2. The dashed lines highlight 50 µM H_2O_2 (horizontal line) and 1.1 x 10^{12} cell L^{-1} (vertical line).

However, there are some confusing experimental results and misinterpretations about the participation and relevance of each intracellular enzyme system in the removal of H_2O_2 that are likely due to experimental limitations [3,9,17,42,43]. Red blood cells pose particular experimental problems related to the presence of a high intracellular concentration of hemoglobin that interfere with many determinations. In fact, the high absorbance of hemoglobin and its interference with fluorescent measurements [44], forces the use of non-physiologic extremely low cell numbers [10,39,44]. Also most experiments require the use of high concentrations of H_2O_2, in the range of 50 µM to 0.5 mM [10,19,39], that combined with a low cell density seem to indicate a negligible role of Prx in H_2O_2 detoxification [9,19].

As demonstrated by experimental results from us (Fig. 2-5) and Low et al [3], as well as by computational simulations (Fig. 6-7), catalase is the main H_2O_2 metabolizing enzyme at cell numbers low enough to allow the use of the fluorescent technique (HRP/pHPA). This is not because of inactivation of Prx, as suggested by other authors [9], but because of a slow recycling rate of the disulfide form of the enzyme when the concentration of H_2O_2 overcome the intracellular concentration of Prx and Trx. In fact, the amount of H_2O_2 consumed by Prx (Q_{Prx}) will depend on the intracellular enzyme concentration, on the cell volume and on the cell number (N) used in each particular setting as given by equation 7 and illustrated in Figure 7B, the remaining H_2O_2 consumption will be mediated mainly by catalase, being minor the contribution of Gpx.

$$Q_{Prx} = \mathrm{Prx\ (M)} \times \mathrm{Vol_{RBC}} \times N \qquad (7)$$

For a typical experiment using the HRP/pHPA system to detect the remaining H_2O_2, the cell density is 3.3 x 10^9 cell L^{-1} and the initial concentration of H_2O_2 is 50 µM. Considering that the RBC volume is 9 x 10^{-14} L [13,14] there will be just 1 x 10^{-7} mole of Prx per liter of cell suspension. Under this experimental condition, the reaction with Prx will account for just a 0.2 % of the total H_2O_2 (50 µM) consumed (Figure 7A). Looking into more details about the metabolism of H_2O_2 in RBC, it should also be noted that the plasma membrane of RBC imposes a significant barrier to permeation. Considering that the rate of the direct bimolecular reaction of Prx with 50 µM H_2O_2 would be 5.9 x 10^{-4} M s^{-1}, if the enzyme were free in solution the reduced form would be totally oxidized in 0.2 ms. However, Prx was active for ~1 s in our simulation (Fig. 6B). The disappearance of the reduced Prx is due to its low recycling rate. In fact, the rate of the reaction between the Cys-51 sulfenic acid (oxidized peroxidatic cysteine) with Cys-172 (resolutive cysteine) is slow (k_3 = 0.64 s^{-1}) [16], but fundamentally the reduction of oxidized Trx back to its reduced form by the NADPH/TR system limits the time frame of action of this multienzyme system. At the same cell density the participation of the GSH/Gpx/GR system starts to be relevant after the Prx system becomes nearly depleted. In this case, the amount of GSH is more than 100 times lower than the added H_2O_2, and although the reductase of GSSG (GR) works at a high rate, Gpx is present at low concentrations in RBC [45]. At very low cell numbers GR uses all cellular NADPH to regenerate GSH, but then the rate of NADPH generation becomes limiting and the consumption by this pathway decreases significantly. The overall contribution of Gpx/GSH/GR system is marginal since it consumes less than ~0.7 % of the H_2O_2 added, as shown in Figure 7. Because the thiol-dependent systems run out quickly, catalase accounts for most (> 97 %) of the H_2O_2 added using cell densities lower than 1 x 10^{10} cell L^{-1}. Since catalase activity does not depend on any other substrate but on H_2O_2 itself and although significantly more slowly than Prx, it can deal with a much greater excess of H_2O_2.

At 3 x 10^{11} cell L^{-1} the effective concentration of Prx is still lower than the concentration of H_2O_2 added, accounting for 25 % of the oxidant (Fig. 6F and 7A). Meanwhile, just 15% of the total peroxide consumption was mediated by the Gpx/GSH/GR system (Fig. 6). At this cell density catalase still decomposes more than 50% of the added H_2O_2, as shown by both simulations (Fig. 6F and 7A) and oxygen production experiments (Fig. 4), in agreement with previous studies performed with 5 x 10^{11} cell L^{-1} [46]. Finally, above 2 x 10^{12} cell L^{-1} and at the average physiologic hematocrit (5 x 10^{12} cell L^{-1}), Prx ensures H_2O_2 removal by direct reaction (Fig. 6I and 7A), confirming its role of non-catalytic H_2O_2 scavenger [3].

Simulations at different cell densities show that there is a time sequence involving Prx as the first line of

defense against H_2O_2, that when it becomes nearly depleted the consumption of H_2O_2 is accomplished by catalase, albeit at a significantly lower rate, with minor contribution from Gpx. As expected, the concentration of H_2O_2 also affects its removal pathway, and Figure 7B was designed to contribute with the proper selection of the cell density and peroxide concentration to investigate the different antioxidant systems.

In conclusion, our findings underscore the importance of considering the cell number carefully because it will determine the effective concentration of enzymes during analysis performed on complex cellular enzyme systems as the one responsible for H_2O_2 metabolism in RBC and provide an easy to follow framework for choosing the experimental conditions that will explore a given enzymatic system in RBC.

Acknowledgements: We are grateful to Dr Gerardo Ferrer-Sueta and Dr Beatriz Alvarez for excellent suggestions and critical discussions.

Funding: This work was partially supported by grants C38-432 from CSIC to AD, and FCE_1_2017_1_136043 to LT and MM. Florencia Orrico is a graduate fellow of CAP-UdelaR.

Conflict of interest: The authors declare that there are no conflicts of interest with the contents of this article.

References

[1] H.J. Forman, A. Bernardo, K.J.A. Davies, What is the concentration of hydrogen peroxide in blood and plasma?, Arch. Biochem. Biophys. 603 (2016) 48–53. doi:10.1016/j.abb.2016.05.005.

[2] M. Trujillo, G. Ferrer-Sueta, L. Thomson, L. Flohé, R. Radi, Kinetics of peroxiredoxins and their role in the decomposition of peroxynitrite, Subcell. Biochem. 44 (2007) 83–113.

[3] F.M. Low, M.B. Hampton, A.V. Peskin, C.C. Winterbourn, Peroxiredoxin 2 functions as a noncatalytic scavenger of low-level hydrogen peroxide in the erythrocyte, Blood. 109 (2007) 2611–2617. doi:10.1182/blood-2006-09-048728.

[4] B. Manta, M. Hugo, C. Ortiz, G. Ferrer-Sueta, M. Trujillo, A. Denicola, The peroxidase and peroxynitrite reductase activity of human erythrocyte peroxiredoxin 2, Arch. Biochem. Biophys. 484 (2009) 146–154. doi:10.1016/j.abb.2008.11.017.

[5] C.-S. Cho, G.J. Kato, S.H. Yang, S.W. Bae, J.S. Lee, M.T. Gladwin, S.G. Rhee, Hydroxyurea-induced expression of glutathione peroxidase 1 in red blood cells of individuals with sickle cell anemia, Antioxid. Redox Signal. 13 (2010) 1–11. doi:10.1089/ars.2009.2978.

[6] A.H. Bryk, J.R. Wiśniewski, Quantitative Analysis of Human Red Blood Cell Proteome, J. Proteome Res. 16 (2017) 2752–2761. doi:10.1021/acs.jproteome.7b00025.

[7] R.B. Moore, M.V. Mankad, S.K. Shriver, V.N. Mankad, G.A. Plishker, Reconstitution of Ca(2+)-dependent K+ transport in erythrocyte membrane vesicles requires a cytoplasmic protein, J. Biol. Chem. 266 (1991) 18964–18968.

[8] R.M. Johnson, Y.-S. Ho, D.-Y. Yu, F.A. Kuypers, Y. Ravindranath, G.W. Goyette, The effects of disruption of genes for peroxiredoxin-2, glutathione peroxidase-1, and catalase on erythrocyte oxidative metabolism, Free Radic. Biol. Med. 48 (2010) 519–525. doi:10.1016/j.freeradbiomed.2009.11.021.

[9] R. Benfeitas, G. Selvaggio, F. Antunes, P.M.B.M. Coelho, A. Salvador, Hydrogen peroxide metabolism and sensing in human erythrocytes: a validated kinetic model and reappraisal of the role of peroxiredoxin II, Free Radic. Biol. Med. 74 (2014) 35–49. doi:10.1016/j.freeradbiomed.2014.06.007.

[10] F. Amen, A. Machin, C. Touriño, I. Rodríguez, A. Denicola, L. Thomson, N-acetylcysteine improves the quality of red blood cells stored for transfusion, Arch. Biochem. Biophys. 621 (2017) 31–37. doi:10.1016/j.abb.2017.02.012.

[11] D.P. Nelson, L.A. Kiesow, Enthalpy of decomposition of hydrogen peroxide by catalase at 25 degrees C (with molar extinction coefficients of H 2 O 2 solutions in the UV), Anal. Biochem. 49 (1972) 474–478.

[12] C. Li, M. Donizelli, N. Rodriguez, H. Dharuri, L. Endler, V. Chelliah, L. Li, E. He, A. Henry, M.I. Stefan, J.L. Snoep, M. Hucka, N. Le Novère, C. Laibe, BioModels Database: An enhanced, curated and annotated resource for published quantitative kinetic models, BMC Syst. Biol. 4 (2010) 92. doi:10.1186/1752-0509-4-92.

[13] E. Evans, Y.C. Fung, Improved measurements of the erythrocyte geometry, Microvasc. Res. 4 (1972) 335–347.

[14] H. Park, S. Lee, M. Ji, K. Kim, Y. Son, S. Jang, Y. Park, Measuring cell surface area and deformability of individual human red blood cells over blood storage using quantitative phase imaging, Sci. Rep. 6 (2016) 34257. doi:10.1038/srep34257.

[15] B. Chance, D.S. Greenstein, F.J.W. Roughton, The mechanism of catalase action. I. Steady-state analysis, Arch. Biochem. Biophys. 37 (1952) 301–321.

[16] S. Portillo-Ledesma, L.M. Randall, D. Parsonage, J. Dalla Rizza, P.A. Karplus, L.B. Poole, A. Denicola, G. Ferrer-Sueta, Differential Kinetics of Two-Cysteine Peroxiredoxin Disulfide Formation Reveal a Novel Model for Peroxide Sensing, Biochemistry (Mosc.). (2018). doi:10.1021/acs.biochem.8b00188.

[17] A.V. Peskin, N. Dickerhof, R.A. Poynton, L.N. Paton, P.E. Pace, M.B. Hampton, C.C. Winterbourn, Hyperoxidation of peroxiredoxins 2 and 3: rate constants for the reactions of the sulfenic acid of the peroxidatic cysteine, J. Biol. Chem. 288 (2013) 14170–14177. doi:10.1074/jbc.M113.460881.

[18] C.C. Winterbourn, D. Metodiewa, Reactivity of biologically important thiol compounds with superoxide and hydrogen peroxide, Free Radic. Biol. Med. 27 (1999) 322–328.

[19] R.M. Johnson, G. Goyette, Y. Ravindranath, Y.-S. Ho, Hemoglobin autoxidation and regulation of endogenous H2O2 levels in erythrocytes, Free Radic. Biol. Med. 39 (2005) 1407–1417. doi:10.1016/j.freeradbiomed.2005.07.002.

[20] L.E. Tomalin, A.M. Day, Z.E. Underwood, G.R. Smith, P. Dalle Pezze, C. Rallis, W. Patel, B.C. Dickinson, J. Bähler, T.F. Brewer, C.J.-L. Chang, D.P. Shanley, E.A. Veal, Increasing extracellular H2O2 produces a bi-phasic response in intracellular H2O2, with peroxiredoxin hyperoxidation only triggered once the

cellular H2O2-buffering capacity is overwhelmed, Free Radic. Biol. Med. 95 (2016) 333–348. doi:10.1016/j.freeradbiomed.2016.02.035.

[21] S. Hoops, S. Sahle, R. Gauges, C. Lee, J. Pahle, N. Simus, M. Singhal, L. Xu, P. Mendes, U. Kummer, COPASI--a COmplex PAthway SImulator, Bioinforma. Oxf. Engl. 22 (2006) 3067–3074. doi:10.1093/bioinformatics/btl485.

[22] M.A. Aon, B.A. Stanley, V. Sivakumaran, J.M. Kembro, B. O'Rourke, N. Paolocci, S. Cortassa, Glutathione/thioredoxin systems modulate mitochondrial H2O2 emission: an experimental-computational study, J. Gen. Physiol. 139 (2012) 479–491. doi:10.1085/jgp.201210772.

[23] C.F. Ng, F.Q. Schafer, G.R. Buettner, V.G.J. Rodgers, The rate of cellular hydrogen peroxide removal shows dependency on GSH: mathematical insight into in vivo H2O2 and GPx concentrations, Free Radic. Res. 41 (2007) 1201–1211. doi:10.1080/10715760701625075.

[24] S. Cortassa, M.A. Aon, R.L. Winslow, B. O'Rourke, A mitochondrial oscillator dependent on reactive oxygen species, Biophys. J. 87 (2004) 2060–2073. doi:10.1529/biophysj.104.041749.

[25] L. Flohé, I. Brand, Kinetics of glutathione peroxidase, Biochim. Biophys. Acta. 191 (1969) 541–549.

[26] D.J. Worthington, M.A. Rosemeyer, Glutathione reductase from human erythrocytes. Catalytic properties and aggregation, Eur. J. Biochem. 67 (1976) 231–238.

[27] R.L. Krauth-Siegel, L.D. Arscott, A. Schönleben-Janas, R.H. Schirmer, C.H. Williams, Role of active site tyrosine residues in catalysis by human glutathione reductase, Biochemistry (Mosc.). 37 (1998) 13968–13977. doi:10.1021/bi980637j.

[28] M. Deponte, Glutathione catalysis and the reaction mechanisms of glutathione-dependent enzymes, Biochim. Biophys. Acta. 1830 (2013) 3217–3266. doi:10.1016/j.bbagen.2012.09.018.

[29] T. Nishino, A. Yachie-Kinoshita, A. Hirayama, T. Soga, M. Suematsu, M. Tomita, In silico modeling and metabolome analysis of long-stored erythrocytes to improve blood storage methods, J. Biotechnol. 144 (2009) 212–223. doi:10.1016/j.jbiotec.2009.08.010.

[30] P.J. Mulquiney, P.W. Kuchel, Model of 2,3-bisphosphoglycerate metabolism in the human erythrocyte based on detailed enzyme kinetic equations: equations and parameter refinement, Biochem. J. 342 Pt 3 (1999) 581–596.

[31] B.M. Pearse, M.A. Rosemeyer, Human 6-phosphogluconate dehydrogenase. Purification of the erythrocyte enzyme and the influence of ions and NADPH on its activity, Eur. J. Biochem. 42 (1974) 213–223.

[32] M. Rippa, P.P. Giovannini, M.P. Barrett, F. Dallocchio, S. Hanau, 6-Phosphogluconate dehydrogenase: the mechanism of action investigated by a comparison of the enzyme from different species, Biochim. Biophys. Acta. 1429 (1998) 83–92.

[33] D.R. Thorburn, P.W. Kuchel, Regulation of the human-erythrocyte hexose-monophosphate shunt under conditions of oxidative stress. A study using NMR spectroscopy, a kinetic isotope effect, a reconstituted system and computer simulation, Eur. J. Biochem. 150 (1985) 371–386.

[34] G. Takebe, J. Yarimizu, Y. Saito, T. Hayashi, H. Nakamura, J. Yodoi, S. Nagasawa, K. Takahashi, A comparative study on the hydroperoxide and thiol specificity of the glutathione peroxidase family and selenoprotein P, J. Biol. Chem. 277 (2002) 41254–41258. doi:10.1074/jbc.M202773200.

[35] C. Giulivi, K.J. Davies, A novel antioxidant role for hemoglobin. The comproportionation of ferrylhemoglobin with oxyhemoglobin, J. Biol. Chem. 265 (1990) 19453–19460.

[36] N.V. Tolan, L.I. Genes, W. Subasinghe, M. Raththagala, D.M. Spence, Personalized metabolic assessment of erythrocytes using microfluidic delivery to an array of luminescent wells, Anal. Chem. 81 (2009) 3102–3108. doi:10.1021/ac900084g.

[37] J.W. Hartz, S. Funakoshi, H.F. Deutsch, The levels of superoxide dismutase and catalase in human tissues as determined immunochemically, Clin. Chim. Acta Int. J. Clin. Chem. 46 (1973) 125–132.

[38] M.R. Fernando, H. Nanri, S. Yoshitake, K. Nagata-Kuno, S. Minakami, Thioredoxin regenerates proteins inactivated by oxidative stress in endothelial cells, Eur. J. Biochem. 209 (1992) 917–922.

[39] B.A. Wagner, J.R. Witmer, T.J. van 't Erve, G.R. Buettner, An Assay for the Rate of Removal of Extracellular Hydrogen Peroxide by Cells, Redox Biol. 1 (2013) 210–217. doi:10.1016/j.redox.2013.01.011.

[40] M. Takahashi, Role of the inflammasome in myocardial infarction, Trends Cardiovasc. Med. 21 (2011) 37–41. doi:10.1016/j.tcm.2012.02.002.

[41] J.B. Lim, B.K. Huang, W.M. Deen, H.D. Sikes, Analysis of the lifetime and spatial localization of hydrogen peroxide generated in the cytosol using a reduced kinetic model, Free Radic. Biol. Med. 89 (2015) 47–53. doi:10.1016/j.freeradbiomed.2015.07.009.

[42] C.-S. Cho, S. Lee, G.T. Lee, H.A. Woo, E.-J. Choi, S.G. Rhee, Irreversible inactivation of glutathione peroxidase 1 and reversible inactivation of peroxiredoxin II by H2O2 in red blood cells, Antioxid. Redox Signal. 12 (2010) 1235–1246. doi:10.1089/ars.2009.2701.

[43] S. Mueller, H.D. Riedel, W. Stremmel, Direct evidence for catalase as the predominant H2O2 -removing enzyme in human erythrocytes, Blood. 90 (1997) 4973–4978.

[44] B.S.S. Anand, N. Sujatha, Fluorescence quenching effects of hemoglobin on simulated tissue phantoms in the UV–Vis range, Meas. Sci. Technol. 23 (2012) 025502. doi:10.1088/0957-0233/23/2/025502.

[45] K. Takahashi, N. Avissar, J. Whitin, H. Cohen, Purification and characterization of human plasma glutathione peroxidase: a selenoglycoprotein distinct from the known cellular enzyme, Arch. Biochem. Biophys. 256 (1987) 677–686.

[46] E. Nagababu, F.J. Chrest, J.M. Rifkind, Hydrogen-peroxide-induced heme degradation in red blood cells: the protective roles of catalase and glutathione peroxidase, Biochim. Biophys. Acta BBA - Gen. Subj. 1620 (2003) 211–217. doi:10.1016/S0304-4165(02)00537-8.